

A CONCEPTUAL DESIGN OF RF SYSTEM IN THE NSP SUPERCONDUCTING LINAC AT JAERI

E. Chishiro, Y. Honda*, N. Ouchi, Y. Touchi**, K. Hasegawa, J. Kusano and M. Mizumoto
 Proton Accelerator Laboratory, Japan Atomic Energy Research Institute
 *Mitsubishi Heavy Industries, Ltd., **Sumitomo Heavy Industries, Ltd.
 Tokai-mura, Naka-gun, Ibaraki-ken, 319-1195 Japan

Abstract

We have performed a conceptual design work of an RF system for a superconducting (SC) linac proposed for Neutron Science Project (NSP) at JAERI. An accelerating structure of the SC linac is divided into 8 different β -sections. The linac has 284-cavities and the length of 690-m. The 8 sections system suppresses the beam emittance growth and reduces the linac length. In the steady state, beam loading for three operation modes is calculated. For a pulse operation with a peak beam current of 30mA (chopping factor of 0.6), the peak RF power of 138kW is required at the high- β cavity. The power of 41kW is required for CW operation at a beam current of 5.33mA. Tuning errors on coupling and cavity resonant frequency are evaluated. In the conceptual design in which an RF power of klystron is distributed to 4-cavities, supply power is estimated. The supply power of about 20 MW is required for both operation modes.

1 INTRODUCTION

The NSP accelerator will consist of RFQ, DTL, Separated-type DTL and SC linac [1]. The SC linac accelerates hydrogen ions from 0.1 to 1.5GeV. It should be operated both in pulse and CW for demands in the applications. This requirement is the essential feature for the RF system. Table 1 shows a preliminary specification for the SC linac. Beam dynamics study has been carried out to determine the SC linac structure. RF system design work is performed under those parameters.

2 SC LINAC STRUCTURE DESIGN

The relative particle velocity (β) gradually increases from 0.43 to 0.92 along the SC linac. Therefore, accelerating cavities are divided into several sections with different β values to match to the particle velocity. The β -section is determined in the view of the bunch phase slip. The SC linac divided by many β -sections has the

Table 1: Preliminary specification of the SC linac

Energy	0.1 to 1.5GeV
Final beam power	8 MW
Accelerating particle	H ⁺ , H ⁺
Frequency	600 MHz
Synchronous phase	-30 degree
Beam operation	1st stage pulse 2nd stage pulse/CW
Peak current	16 mA at 1st stage 30 mA at 2nd pulse mode 5.33 mA at CW mode
Repetition rate	50 Hz
Macro pulse width	2 to 5.9 ms, CW
Intermediate pulse width	400 ns (interval 270 ns)

advantage of accelerating efficiency and less emittance growth because of the less phase slip. For the capital and maintenance cost, number of sections should not be increased so much.

Prior to the β -section decision, basic parameters were prepared [2]. The number of cells per cavity is 5. The peak surface electrical field (E_{peak}) is limited to be 16 MV/m. The cavity surface resistance is estimated to be 15 n Ω . The number of cavities excited by an amplifier is set to be 4. It is indicated that the 4 cavities are fed with the same RF power.

The number of β -sections is decided by considering the RMS emittance growth and the linac length [3]. As the result of the study, the length and the emittance growth can be saturated over 8 β -sections. In the conceptual design, we chose the linac structure with 8 β -sections. The diagram is shown in Fig. 1 and its RF parameters are listed in Table 2. The linac has 284-cavities and the 690-m length.

3 STEADY-STATE BEAM LOADING

We calculated the required peak RF power in the steady state for each operation modes. The required power (P_f) is given by [4]

$$P_f = \frac{(1 + \beta_c)^2 V_{\text{acc}}^2}{4\beta_c R} \times \left\{ (1 - \tan \psi_b / \tan \phi)^2 + (\tan \psi_c - \tan \psi_b)^2 \right\} \quad (1)$$

where β_c is the coupling factor to the cavity, ϕ is the synchronous phase and R is the cavity shunt impedance defined by $R = V_{\text{acc}}^2 / (\text{cavity wall loss})$. Beam-loading detune angle (ψ_b) and cavity detuning angle (ψ_c) are defined by following equations, respectively.

$$\tan \psi_b = -\frac{R \cdot I_b}{(1 + \beta_c) V_{\text{acc}}} \sin \phi, \quad (2)$$

$$\tan \psi_c = \frac{\omega_c - \omega_{\text{rf}}}{\omega_c} \frac{2Q_0}{1 + \beta_c}, \quad (3)$$

where I_b is beam current, ω_c is cavity resonant frequency, ω_{rf} is driven frequency and Q_0 is unloaded Q value. To minimize the P_f , those angles have to be set to $\psi_b = \psi_c = -\phi$. Therefore, the optimum β_c and ω_c are obtained by

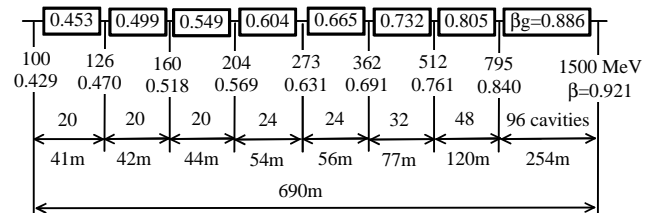


Figure 1: Diagram of Linac structure

Table 2: Design parameters of SC linac

Section No.	1	2	3	4	5	6	7	8
β	0.43 -0.47	0.47 -0.52	0.52 -0.66	0.57- 0.63	0.63 -0.69	0.69- 0.76	0.76 -0.84	0.84 -0.92
Vacc (MV/cav.)*	1.34- 1.60	1.78- 2.11	2.35- 2.74	3.03- 3.56	3.96- 4.51	4.95- 5.69	6.26- 7.13	7.85- 8.82
TTF	0.53 -0.65	0.55-0.67	0.58- 0.69	0.60- 0.71	0.62- 0.72	0.63-0.73	0.64-0.73	0.66 -0.74
Q_0	8.31E9	9.16E9	1.01E10	1.11E10	1.22E10	1.32E10	1.44E10	1.57E10
R/Q (Ω /cav.)	38.5- 58.5	58.8- 86.4	86.6- 122	121- 170	172- 227	223- 295	289- 377	370- 470

* Cavity accelerating voltage = Average electric field x Cavity length x TTF (Transit Time Factor)

$$\beta_{\text{copt}} = 1 + \frac{RI_b \cos \phi}{V_{\text{acc}}}, \quad (4)$$

$$\omega_{\text{copt}} = \omega_{\text{rf}} \left\{ 1 - \frac{I_b}{2V_{\text{acc}}} (R/Q_0) \sin \phi \right\}. \quad (5)$$

Under the optimum condition, the required power is given by $P_{\text{fopt}} = (1 + \beta_c)^2 V_{\text{acc}}^2 / (\beta_c R)$.

In the SC cavity, the required RF power is almost the same as beam loading under the optimum condition. The required power is shown in Fig. 2. The power is gradually increasing with the cavity number and the power at the high- β end is 6.6 times as large as that at the low- β end. For the pulse operation, the maximum power of 138 kW/cav. is needed at the high β -section. On the other hand, the power of 41 kW/cav. is required for the CW operation. There is difference of 3.4 times in the power between CW and pulse operations. The RF system including tuner, coupler, amplifier and so on have to manage this difference.

Tuning errors on β_c and ω_c cause the increase of the required RF power. Those tuning errors are evaluated for the SC linac. Figure 3 shows the dependence of the power enhancement on the coupling error (normalized by the optimum power P_{fopt} and the coupling factor β_{copt}). For the coupling error of $\pm 30\%$, the power to keep the V_{acc} in the cavity increases 1.7% at over coupling and 3.2 % at under coupling. The coupling error does not seriously affect the power enhancement.

The cavity tuning error is evaluated for the cavity detuning angle (ψ_c). Figure 4 shows the dependence of the power on the ψ_c . The power is minimized at $\psi_c = 30$ degree ($=\psi_b$). Over the 30 degree, the power is rapidly

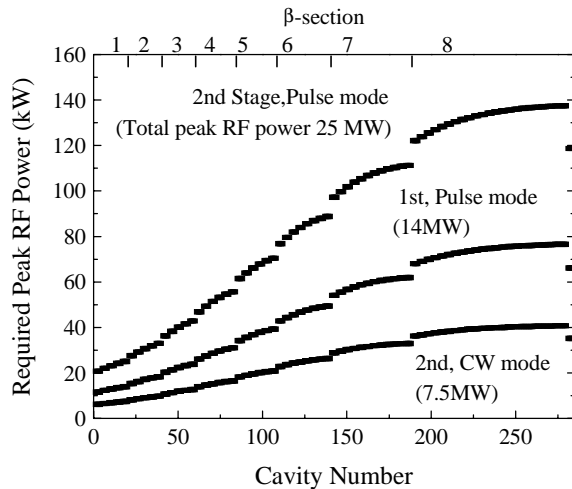


Fig. 2: Peak RF Power Requirement for the SC Linac

increased. For the shift of ± 30 degree from the optimum detuning angle, the power increases 8 % at -30 degree shift and 33 % at $+30$ degree. Using the parameters seen in Table 2 and the described equations, resonant frequency error of the cavity #1 at the 2nd stage CW mode is calculated. The tuning error of ± 30 degree corresponds to the resonant frequency error of -24 Hz and $+47$ Hz, respectively. The precise tuning is needed for the cavity pre-detuning.

4 RF SYSTEM OF SC LINAC

4.1 Klystron

The design study of the RF system has been performed on the basis on klystrons, which are well suited to accelerator use. In the SC linac RF system, the klystron has to operate in the high power pulse mode and low power CW mode. In addition, the klystron also has to cover wide power range because of varying the required power along the SC linac. We have selected the klystron with modulating anode. Klystrons with property of UHF-band (508 MHz), high power (1MW) and CW operation have been already operated in TRISTAN and SPring-8. The maximum power satisfies our request (138kWx 4cavites + α).

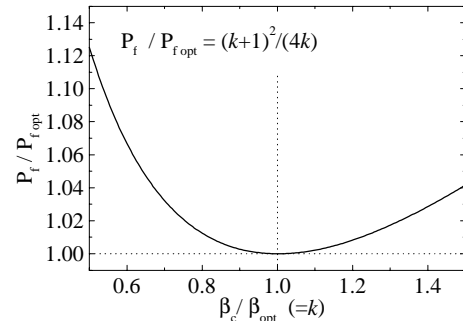


Fig 3: Required Power Enhancement for Coupling Error

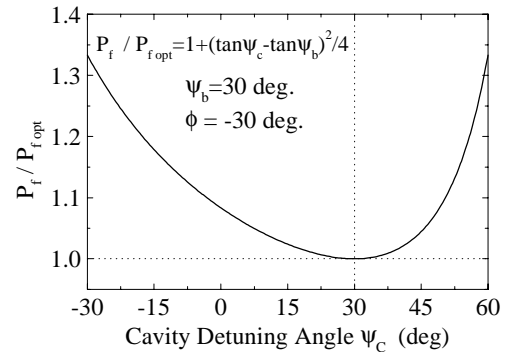


Fig 4: Power Enhancement for Cavity Detuning Error

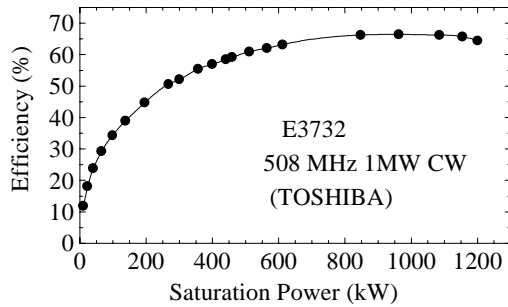


Fig.5: Efficiency Characteristic of the Klystron

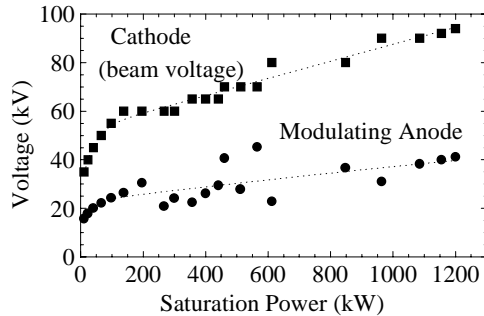


Fig.6: Cathode and Anode Voltage for Saturation Power

Klystron is manufactured such that its maximum efficiency becomes at the full saturation power. When the klystron operates below the saturation, the efficiency falls if the klystron beam power is not reduced. To keep higher efficiency in the low power range, the beam voltage is reduced. We have measured the efficiency characteristics using a 508 MHz klystron (E3732, TOSHIBA). Figure 5 shows dependence of the efficiency on the saturation power. Figure 6 shows the cathode and anode voltage where the power is saturated, respectively. The efficiency below 50% is measured at the power of 250 kW or less.

4.2 System efficiency and supply power

The RF system efficiency and supply power are estimated on the basis of the characteristic seen in Fig 5[5]. The result is given in Table 3. Since the klystron drives the 4-cavities, klystrons of 71 unit are needed in the RF system. High power tubes (44 units) with 1MW output and low power tubes (27units) with 400 kW are arranged in the linac to cope with the varying RF power requirement along the linac. To control the cavity field, some amount of RF margins are necessary. In this design, the margin of 15% is assumed. Considering power loss of 5 % in the transmission line, the klystrons are operated at 80% for the saturation power. Therefore operation efficiency becomes 0.8 times of saturation efficiency.

In the 2nd stage pulse operation, maximum output power of 690 kW (138 kW x 4 cavities x 1/0.8) is required at high β -end klystron. Since the efficiency at the saturation power is 64 % (see in Fig. 5), operating efficiency is estimated to be 51 % (64 % x 0.8). The supply power to the klystron is calculated to be 1082 kW (138kW x 4 cavities / 0.51 %).

The estimation is carried out for the klystrons of 71 units at each operation mode. At CW operation, averaged klystron efficiency is 33% due to operate the klystrons at

low power. Averaged supply power is calculated to take into account the duty including time to rise field in the cavity. The averaged supply power to the RF system needs of about 20 MW for both of CW and pulse mode at the 2nd stage.

4.3 IOT system

Another choice of the SC linac RF system is a scheme that one-cavity is driven by one-IOT (Inductive Output Tube). This system is regarded as a suitable system for an RF control. In addition, the IOT is compact and is kept with high efficiency at low output power. In a rough estimation, the supply power at CW operation is reduced to 14 MW. However, high power IOT (more than 120kW) does not exist at present. In the case that the IOT is applied as all amplifiers, 568 tubes including pre-amplifiers are needed. Using many tubes may cause decrease of accelerator reliability. At present, we have done the preparation to evaluate the performance of a CW-35 kW IOT.

5 CONCLUSION

The SC linac with 8 β -sections is determined in the view of the bunch phase slip with respect to the RF phase in the cavity. This linac is an effective option for its shorter length and lower emittance growth. In steady state, the beam loadings under the optimum conditions were calculated. The maximum RF power requirements of 138kW at pulse operation and 41kW at CW operation are estimated. As a result of consideration on the tuning error, the precise tuning is needed for the cavity pre-detuning. In the conceptual design there the output power of a klystron is distributed to 4-cavities, the averaged supply power is estimated. The powers of about 20 MW are needed for both operation modes at 2nd stage.

Table 3: Efficiency and Supply Power in the RF System

Operation Mode	1st		2nd stage
	Pulse	Pulse	CW
Beam pulse width (ms)	2	5.9	cw
Peak RF power (MW)	14	25	7.5
Klystron efficiency (%)	41	48	33
Peak supply power (MW)	34	53	23
Averaged duty *	0.18	0.38	1
Averaged supply power (MW)	5.8	20	23

* Including time to rise field in cavity

REFERENCES

- [1] M. Mizumoto et al., "High Intensity Proton Accelerator for Neutron Science Project at JAERI", Proc. of EPAC98, Stockholm, June 22-26, (1998).
- [2] N. Ouchi et al., "Proton Accelerator Activities in JAERI", Proc. of the 8th Workshop on RF Superconductivity, Italy (1997).
- [3] Y. Honda et al., "A Conceptual Design Study of Superconducting Proton Linear Accelerator for Neutron Science Project", Proc. of 1st APAC, KEK, March 23-27, (1998).
- [4] T. P. Wangler, "Principles of RF Linear Accelerators", John Wiley & Sons Inc., (1998).
- [5] E. Chishiro et al., "An RF Power System for NSP High Intensity Proton Accelerator at JAERI", Proc. of 1st APAC, KEK, March 23-27, (1998).